NIH Public Access
Author Manuscript
J Proteome Res. Author manuscript; available in PMC 2008 November 3.

Published in final edited form as:
J Proteome Res. 2007 February ; 6(2): 759–771. doi:10.1021/pr060383l.

Quantitative Proteomic and Microarray Analysis of the Archaeon *Methanosarcina Acetivorans* Grown with Acetate *Versus* Methanol*

Lingyun Li[‡,§], **Qingbo Li**[¶,§,‖], **Lars Rohlin**[†,§], **UnMi Kim**[†], **Kirsty Salmon**[†], **Tomas Rejtar**[‡], **Robert P. Gunsalus**[†], **Barry L. Karger**[‡], and **James G. Ferry**[¶,#]

‡*Barnett Institute and Department of Chemistry, Northeastern University, Boston, MA 02115*

¶*Department of Biochemistry and Molecular Biology, and Center for Microbial Structural Biology, 205 South Frear Laboratory, The Pennsylvania State University, University Park, PA 16802*

†*Department of Microbiology, Immunology, and Molecular Genetics, and the Molecular Biology Institute, University of California, Los Angeles, CA 90095*

Summary

Methanosarcina acetivorans strain C2A is an acetate- and methanol-utilizing methane-producing organism for which the genome, the largest yet sequenced among the Archaea, reveals extensive physiological diversity. LC linear ion trap-FTICR mass spectrometry was employed to analyze acetate- *vs.* methanol-grown cells metabolically labeled with ^{14}N *vs.* ^{15}N, respectively, to obtain quantitative protein abundance ratios. DNA microarray analyses of acetate- *vs.* methanol-grown cells was also performed to determine gene expression ratios. The combined approaches were highly complementary, extending the physiological understanding of growth and methanogenesis. Of the 1081 proteins detected, 255 were ≥ 3-fold differentially abundant. DNA microarray analysis revealed 410 genes that were ≥ 2.5-fold differentially expressed of 1972 genes with detected expression. The ratios of differentially abundant proteins were in good agreement with expression ratios of the encoding genes. Taken together, the results suggest several novel roles for electron transport components specific to acetate-grown cells, including two flavodoxins each specific for growth on acetate or methanol. Protein abundance ratios indicated that duplicate CO dehydrogenase/acetyl-CoA complexes function in the conversion of acetate to methane. Surprisingly, the protein abundance and gene expression ratios indicated a general stress response in acetate- *vs.* methanol-grown cells that included enzymes specific for polyphosphate accumulation and oxidative stress. The microarray analysis identified transcripts of several genes encoding regulatory proteins with identity to the PhoU, MarR, GlnK, and TetR families commonly found in the Bacteria domain. An analysis of neighboring genes suggested roles in controlling phosphate metabolism (PhoU), ammonia assimilation (GlnK), and molybdopterin cofactor biosynthesis (TetR). Finally, the proteomic and microarray results suggested roles for two-component regulatory systems specific for each growth substrate.

Keywords

Quantitative proteomics; metabolic labeling; microarray; methanogenesis; acetate; methanol

#To whom correspondence should be addressed. Tel.: 814/863-5721; Fax: 814/863-6217; E-mail: jgf3@psu.edu.
§Each contributed equally.
‖Present address: Department of Microbiology and Immunology, University of Illinois at Chicago, Chicago, IL 60607-7173.

NIH-PA Author Manuscript
NIH-PA Author Manuscript
NIH-PA Author Manuscript

NIH-PA Author Manuscript

NIH-PA Author Manuscript

NIH-PA Author Manuscript

Introduction

The microbiological conversion of organic matter to methane in diverse oxygen-free (anaerobic) environments is an important link in the global carbon cycle [1]. The same process is employed for methane formation from biological waste and plant biomass (biomethanation), an alternative to fossil fuels [2]. In the process, fermentative and acetogenic anaerobes convert the complex biomass to acetate, formate, CO_2, and H_2, such species being utilized for growth of methane-producing (methanogen) species by two distinct pathways [3]. In the CO_2-reduction pathway, either formate or H_2 is oxidized which in turn provides electrons for the reduction of CO_2 to methane. In the acetate fermentation pathway, acetate is cleaved, and the methyl group is reduced to methane with electrons derived from oxidation of the carbonyl group to CO_2. Methanol, and other simple methyl-containing compounds, are also growth substrates for methylotrophic methanogens found in specialized anaerobic environments. The pathway for methane formation is a dismutation of the substrate in which methyl groups are either oxidized to CO_2, generating reducing potential, or reduced to methane. Global proteomic and DNA microarray analyses have contributed to the understanding of diverse physiological aspects of species metabolizing methylotrophic substrates [4-13] or reducing CO_2 [14-21] to methane; however, few comprehensive global analyses of acetate metabolism are reported [10, 11].

Approximately two-thirds of the methane in nature derives from the fermentation of acetate by one of two genera, *Methanosarcina* and *Methanosaeta*. Thus, an understanding of growth and methane formation from acetate is essential to understanding the native ecology, and development of process parameters for control and optimization of the large-scale biomethanation of renewable plant biomass. Key to this understanding is the identification of proteins essential for acetate-dependent growth and methane formation. Several proteins have been discovered by either proteomic or DNA[1] microarray approaches comparing acetate- vs. methanol-grown *Methanosarcina* species. DNA microarray analyses of the freshwater isolate *Methanosarcina mazei*[11] has identified genes up regulated in response to growth with acetate *vs.* methanol, suggesting roles for the encoded proteins specific to each pathway.

Methanosarcina acetivorans is a marine isolate for which the genome, the largest yet among the Archaea, has been sequenced,[22] suggesting extensive metabolic diversity. Several tools for genetic manipulation have been developed for *M. acetivorans*[23-26] and the application of these tools exquisitely documented [27-29]. Thus, *M. acetivorans* is particularly suited for investigation of the physiology of acetate-dependent growth and methanogenesis. A limited proteomic analysis of acetate- *vs.* methanol-grown *M. acetivorans*[30] has revealed differences in the electron transport pathways of acetate-grown cells compared to *M. mazei*[11].

A combined proteomic and DNA microarray approach to investigate any *Methanosarcina* species has not been reported. Here, we present a comprehensive quantitative analysis of the proteome, complemented by transcrptome analysis, of acetate- *vs.* methanol-grown *M. acetivorans*. In general, good agreement was observed between the proteomics and microarray data. The more advanced proteomic analyses combined with the microarray results provide a much larger and complementary in depth view of acetate and methanol metabolism that includes features of electron transport, regulation, and the general stress response.

[1]The abbreviations used are: DNA, deoxyribonucleic acid; NCBI, National Center for Biotechnology Information; RT, reverse transcriptase; DNase, deoxyribonuclease; dATP, deoxyadenosine triphosphate; dCTP, deoxycytidine triphosphate; dGTP, deoxyguanosine triphosphate; dTTP, deoxythimadine triphosphate; dUTP, deoxyuridine triphosphate; RNase, ribonuclease; cDNA, complementary deoxyribonucleic acid; MCMC, Markov Chain Monte Carlo; COG, clusters of orthologous groups; THMPT, tetrahydromethanopterin.

NIH-PA Author Manuscript

NIH-PA Author Manuscript

NIH-PA Author Manuscript

Materials and Methods

Cell growth for proteomic studies

M. acetivorans acetate- and methanol-grown cells were cultured similar to that previously described, [31]. The mineral medium contained in grams per liter: NaCl, 11.69 g; $MgSO_4 \cdot 7H_2O$, 12.32 g; KCl, 0.76 g; $CaCl_2 \cdot 2H_2O$, 0.14 g; NH_4Cl, 0.5 g; Resazurin solution (1000 ×), 1ml; trace metal solution (100X) 10 ml [32]; vitamin solution (100×) 10 ml [32]; HCl (concentrated) 0.5ml; $Na_2HPO_4 \cdot 7H_2O$, 1.12 g; cysteine·HCl·H_2O, 0.25 g; Na_2CO_3, 3.0 g. Methanol-grown cells were substituted with $^{15}NH_4Cl$ (98%) (Sigma, St. Louis, MO). An atmosphere (80:20) of nitrogen to carbon dioxide was used in the head-space. Cells from both cultures were harvested in mid-exponential growth at an OD_{600} of 0.8 and 0.6 for acetate and methanol cultures, respectively, as previously described [31].

Protein extraction, SDS/PAGE fractionation, and in-gel digestion

The cell pellet from about 40 ml of culture was re-suspended in 100 μl of 10 mM Tris-HCl containing 5 mM $MgCl_2$ and 100 U DNase (Roche, Indianapolis, IN), and incubated on ice for 20 min. This treatment was followed by the addition of 900 μl of 8 M urea containing 0.05% SDS, and vortexing for 3 min. The whole cell lysate was cleared by centrifugation at 13,000 × g for 20 min at 4°C. The concentrations of whole-cell protein extracts, determined by the Bradford assay (Bio-Rad, Hercules, CA), from acetate- and methanol-grown cells were 5.8 and 3.5 mg/ml, respectively.

Whole-cell extracts of acetate- and methanol-grown cells were combined to generate a 1:1 (w/w) mixture of the ^{14}N and ^{15}N labeled proteins. An aliquot containing 40 μg of the mixture was diluted to 45 μl with SDS/PAGE sample buffer, consisting of 2% (w/v) SDS, 25% (v/v) glycerol, 100 mM DTT, 0.01% bromophenol blue, and 62.5 mM Tris-HCl (pH 7). The sample was resolved in a precast 12-well 10.5-14% linear gradient Criterion Tris-HCl gel (BioRad, Hercules, CA) developed at 160 V for 50 min. The gel was stained with silver as previously described [33]. The lanes were cut into ten fractions, each of which contained roughly the same total density as estimated by visual inspection aided with a translucent illuminator. Each fraction was separately minced into ~ 1 mm^3 cubes and subjected to washing, in-gel digestion, and peptide extraction steps as described [34] except that the volume of solution added for each step was adjusted to accommodate the volume of gel pieces for each SDS/PAGE fraction. Sequencing grade trypsin (Promega, Madison, WI) was used as the digestion enzyme. The collected peptide extract solution for each fraction (~1.2 ml) was concentrated to ~30 μl final volume in a SPD1010 SpeedVac system (Thermo Savant, Holbrook, NY) at 45°C in a 1.5-ml microcentrifuge tube.

Protein identification and abundance ratio determination

Proteins were identified from the peptide extract of each 1D-SDS/PAGE gel fraction using a shotgun proteomics strategy similar to that previously described [35]. Approximately 10 μl of peptide extract solution was loaded onto a 100 μm × 15 cm column packed with MagicC18 5 μm particles (Michrom BioResources, Auburn, CA), followed by a 75 min linear gradient of 2% to 35% ACN (v/v) in 0.1% formic acid using 300 nl/min flow rate. A hybrid linear ion trap - FTICR instrument (LTQ FT MS,ThermoFinnigan, San Jose, CA) was used for the analysis. In one data acquisition cycle, a single high resolution FT scan with accumulation of up to 2×10^6 ions was followed by acquisition of MS/MS spectra using the linear ion trap (accumulation of 3×10^4 ions) for up to the 7 most intense ions with the dynamic exclusion set to 1 min. A single data acquisition cycle was completed in approximately 3.5 sec. Each 1D-SDS/PAGE fraction was analyzed twice. The acquired data was searched against the NCBI database of *M. acetivorans* C2A in two separate Sequest searches, one corresponding to ^{14}N and the other to ^{15}N labeling. The precursor ion mass tolerance was set to ±1.4 Da, and trypsin was designated

NIH-PA Author Manuscript

NIH-PA Author Manuscript

NIH-PA Author Manuscript

as the proteolytic enzyme with up to 2 missed cleavages. Peptides identified with Xcorr values greater than 1.5 (1+), 2.0 (2+), and 2.5(3+) in either ^{14}N or ^{15}N searches in two replicate LC-MS runs were initially selected, then only peptides with the precursor mass tolerance of ±10 ppm were accepted for quantitative analysis. In about 15% of peptide identifications, the second isotope was initially assigned as the precursor ion, resulting in 1 Da mass shift. In these cases, the shift was corrected for the monoisotopic peak before applying the 10 ppm precursor mass accuracy restriction. Relative abundance of identified peptides was then calculated using a lab-developed program [36] that determined ratios of chromatographic peak areas of the isotopically labeled peptide pairs. For successful quantitation, coeluting ^{14}N, ^{15}N pairs of peptides, with at least one peptide being identified using the database search criteria specified above and the mass difference between the peptides corresponding to the number of nitrogen atoms in the peptide sequence, had to be found. In the next step, the relative abundance ratios of proteins were calculated by averaging of identified peptide abundance ratios. Finally, only proteins quantitated with at least two peptides and protein probabilities greater than 0.95, estimated by Protein Prophet [37], were selected. Importantly, the combination of precursor mass tolerance (±10 ppm), Sequest Xcorr values the presence of a pair of co-eluting peaks, and ProteinProphet probabilities of 0.95 or higher provided highly confident protein identifications.

Cell growth for microarray experiments

M. acetivorans C2A was cultivated on a mineral medium identical to that described for proteomic studies. Following sterilization, the medium was supplemented with filter sterilized 0.1 ml 50 % methanol or 0.2 ml 5 M acetate per 10 ml medium.

For microarray experiments, eight independent cultures of *M. acetivorans* C2A cells were grown with either acetate (six) or methanol (two) with serial transfer (3 times to mid-exponential phase) to achieve steady state cell growth conditions. Cells were then harvested for RNA purification at mid-exponential growth (OD_{600} of 0.2 for acetate grown cultures and OD_{600} of 0.4 for the methanol grown cultures) as previously described [38]. Duplicate samples of RNA from three individual acetate grown cultures were combined, since a lower cell yield was obtained relative to methanol cell growth.

Microarray probe selection and PCR primer design

Probes were designed, generated, and archived as previously described [39]. The product sizes were generally 200 to 300 bp where a total of 3,981 ORFs were represented. Although *M. acetivorans* contains a total of 4,524 ORFs [22], unique PCR products could generated for 3,981 of the ORFs due to presence of multiple homologs of some ORFs; transposases, hypothetical proteins, and some uncharacterized proteins. These ORFs totaled 543 due to high DNA sequence similarity. The RT-PCR primers were created by a modified version of MyPROBES [38]. The PCR product lengths were set to a range of 100-200 bp, melting temperature range 55-66°C, guanine plus cytosine content 55-65%, primer length 17-22 bases.

PCR amplification of microarray probes

PCR products were amplified from chromosomal DNA using the custom designed oligonucleotide pairs at an annealing temperature of 54°C for 30 s. The reactions were then extended for 30 s by *rTaq Polymerase* in 50μl reactions. Each original PCR product was then size verified by agrarose gel electrophoresis where only a singe product of the anticipated size was obtained in most cases. Where multiple bands were obtained, the correct sized fragment was selected by gel purification (QiaQuick Gel Purification Kit) for subsequent use. When no PCR product was obtained in the first round, temperature gradient PCR was performed in order to generate the desired DNA fragment. For the few remaining ORFs that failed using this approach, new oligonucleotides pairs were designed and used in a second attempt to generate the desired PCR product.

NIH-PA Author Manuscript

NIH-PA Author Manuscript

NIH-PA Author Manuscript

For the second round of DNA amplification, each of the initial amplified products (3933 ORFs) were used as templates and the gene specific primers to allow for more uniform product yield. Each PCR fragment was size verified and stocked for DNA cleanup. Prior to slide printing, each PCR generated DNA product was purified using Qiagen columns in a 96-well format (QiaQuick 96-well PCR Purification Kit). The purified DNA was quantified by UV spectrophotometry in 384-well format, and the concentration of each DNA level was determined. For slide printing, 2.4 μg of PCR product resuspended in 10μl 3xSSC with 0.0001% SDS solution was aliquoted into 384 well plates and dried. The remaining DNA was archived for future use in slide printing.

Microarray spotting

PCR products contained in 384 well plates were spotted onto GAPS II slides (Corning, Corning, New York) using a robotic arrayer Virtek ChipWriter Pro (Bio-Rad, Hercules, CA). The diameter of each spot was approximately 150 μm, and the distance between the centers of each spot was 220 μm. Slides were hydrated with steam for 2-3 s and snap dried on a 100°C heating block. The probes were cross-linked to the surface of the slide by UV light (Stratalinker, Stratagene, La Jolla, CA) at 250 mJ and the slides were then baked at 80°C for 3 hours. To minimize background, the slides were blocked by soaking for 15 min in 250 ml of 1-methyl-2-pyrrolidone with 4 g of succinic anhydride and 28 ml of 0.2 M sodium borate solution (pH 8.0). After blocking, the slides were washed with 95°C water for 2 min and transferred to 95% ethanol at room temperature for 1 min prior to drying by centrifugation.

Microarray experimental design

Cultures (10 ml) were incubated in anaerobic tubes at 37°C on a roller for 16-24 h to an OD_{600} of 0.4 for methanol and 70-80 h to an OD_{600} of 0.2 for acetate. Each tube was quick cooled in an ethanol/dry ice bath, cells were harvested by centrifugation with a Sorval ss-34 rotor (2000 rpm at 4°C), and resuspended in RNAlater (Ambion, Austin, TX) as previously described [38]. Each cell growth condition was repeated two times. For microarray calibration, RNA samples from same culture were divided in half, labeled with Cy3 and Cy5 dyes (Amersham) and hybridized to 2 slides each. This calibration experiment was performed twice for each condition to obtain a reference distribution in the data analysis [40, 41].

RNA purification and labeling

For microarray experiments, total RNA was purified from 10 ml of cell samples using the RNAwiz (Ambion, Austin, TX) following the manufacturer's instructions. The purified RNA was treated with DNase I as described [42]. Total RNA (60 μg) was labeled using indirect labeling with amino allyl-dUTP with either Cy3 or Cy5 monofunctional NHS-ester (Amersham Bioscience, Piscataway, NJ). The reverse transcription mixture, (40μl) including 600 units of Superscript II RNase H reverse transcriptase (Invitrogen), 4.5 μg random hexamers, 0.5 mM dATP, dCTP, and dGTP, 0.2 mM dTTP, and 0.3 mM aadUTP (Sigma, St. Louis, MO), was incubated at 42°C for 3 h. The Superscript enzyme was added in two steps, 300 units at time 0 h and 300 units after 1.5 h. After reverse transcription, the RNA was hydrolyzed by incubating at 65°C for 40 min after adding 10 μl of 0.5 M EDTA (pH 8.0) and 10 μl of 1 N NaOH. The cDNAs were neutralized with 25 μl 1M HEPES and purified with a Microcon-30 and dried. The dried cDNA was resuspended in 5 μl water plus 5 μl of 0.1M sodium bicarbonate, and transferred to a dry aliquot of the dye for the coupling reaction. The acetate samples were labeled with Cy3 and methanol were label with Cy5. The coupling reaction was quenched by adding 4.5 μl of 4 M hydroxylamine. The two dye-labeled cDNAs were combined, purified using a Qia-quick column (Qiagen, Valencia, CA), and concentrated to 1-2 μl using a Microcon-30 concentrator (Millipore).

NIH-PA Author Manuscript

NIH-PA Author Manuscript

NIH-PA Author Manuscript

Hybridization, scanning and data analysis

The concentrated Cy3 and Cy5 cDNA was hybridized and washed as described [42]. The dried slides were analyzed using an Agilent DNA microarray scanner at 10 μm. The scanner creates a Tiff file for each channel, Cy3 and Cy5 where two images were simultaneously analyzed in an image analysis program Imagene5 (Biodiscovery, Marina Del Ray CA) to find spot intensities. Microarray spot intensity data were normalized and the 95% confidence level were estimated using the software lcDNA (http://receptor.seas.ucla.edu/lcDNA) [40, 41]. Spot signals less than twice the mean background signal were removed. Outliers were then removed using a quality filtering routine, and the data were normalized using a rank-invariant method [41]. The normalized data were then subjected to the Markov Chain Monte Carlo (MCMC) analysis method [40, 41].

Results and Discussion

Proteomic analysis

Previous 2-D gel MALDI TOF/TOF MS proteomic analyses of *M. acetivorans* identified 412 proteins [31] of which 34 were statistically differentially abundant between acetate- and methanol-grown cells [43]. To obtain a deeper qualitative and quantitative analysis of the proteome, we first separated the lysate by SDS PAGE into 10 fractions and then utilized LC linear ion trap-FTICR MS to analyze acetate- *vs.* methanol-grown cells metabolically labeled with ^{14}N *vs.* ^{15}N, respectively. Each gel fraction was analyzed twice by LC/MS. Using a conservative criterion (≥3-fold change) [44], 255 out of the 1081 quantitated proteins were found to be differentially abundant (≥3-fold change) between acetate- and methanol-grown cells as determined with two or more peptide pairs (Tables 1 and S1). These differentially abundant proteins were considered candidates for roles specific to growth with either methanol or acetate. Of the 255 proteins, 71 were more abundant in acetate- *vs.* methanol-grown cells, whereas 184 were more abundant in methanol- *vs.* acetate-grown *M. acetivorans* (Table 2).

DNA microarray analysis

Transcript profiling of acetate- *vs.* methanol-grown *M. acetivorans* was performed to complement the proteomic results. The cells used for microarray and proteomic analyses were cultured independently which provided biological replicates. Total RNA was isolated from cells following flash cooling (Materials and Methods), and cDNA was then prepared for each experimental condition and used to hybridize to each of two slides. The experimental protocol was repeated to give a total of four slides and a total of eight measurements for each ORF. The data were analyzed using lcDNA, a MCMC method estimating the confidence level of the data, and outliers were removed by a quality filtering routine (Materials and Methods). The normalized data were then subjected to the MCMC analysis method. Of the 3940 spotted genes, 1972 (ca. 50%) had measurable transcript levels under both growth conditions that were two-fold above the mean (data not shown). Of 410 genes showing 2.5-fold or greater differential expression, 200 were expressed greater in response to growth with acetate, and 210 greater in response to methanol (Tables 1 and S1). Due to a higher confidence level of ratios for microarray data, gene expression ratios with a cut-off of ≥2.5-fold were considered candidates for roles specific to growth with either substrate.

Comparison of proteomic and microarray results

A combined total of 577 gene transcripts or proteins were identified by the two approaches (Tables 1 and S1). A comparison of the approaches are shown in Table 2. Of the 255 proteins detected with at least 3-fold differential abundance, 88 of the encoding genes showed a differential expression of 2.5-fold or greater. Of these 88 genes, the expression ratios of 80 were consistent with the protein abundance ratios indicating good agreement between the two

NIH-PA Author Manuscript

NIH-PA Author Manuscript

NIH-PA Author Manuscript

methods of analysis. Microarray analyses detected 322 differentially expressed genes for which the protein products were either not detected or less than 3-fold differentially abundant in the proteome. Conversely, proteomic analyses detected 167 differentially abundant proteins for which transcripts of the encoding genes were not detected or the gene expression ratios were less than 2.5-fold. Some of these differences undoubtedly arise from the thresholds arbitrarily set, while other differences are from the inherently different experimental and biological variables of the two methodologies. Nonetheless, the two methods validate and complement each other, and in a number of cases demonstrate similar trends. Indeed, the combined analysis of experimental data sets provides a superior view of the complex physiology of *M. acetivorans* relative to either approach alone.

As shown in Figure 1, the 577 genes for which both proteomic and genomic microarray data were obtained revealed a reasonable correlation coefficient (R = ~0.61). Only the data with no error measurement associated with it, or where the calculated protein abundance ratio was smaller than its standard deviation (i.e., 30 ± 50), were removed prior to plotting. Finally, three outlier microarray data points were removed where prior RT-PCR data indicated probe errors due to high nucleotide identity of several gene probes. Since the majority of the genes revealed by the two experimental approaches were in reasonably good agreement (R = ~0.61), this result suggests that modulation of gene expression is a major level of control for substrate-specific growth. It is interesting to speculate that divergence of the corresponding proteomic and microarray data identifies potential candidates for regulatory control at the post-transcriptional level. Further experiments are needed to test this notion.

The genes presented in Tables 1 and S1 were classified using the COG functional classification (Table 3). For the genes identified by microarray analysis of acetate-grown cells, two functional categories that were statistically over or under represented were “energy production and conversion” and “replication, recombination and repair”, respectively. The former gene group suggests that a greater number of genes are needed to derive energy from acetate relative to methanol. The latter group is consistent with a reduced rate of cell replication with acetate relative to methanol. A similar COG group pattern was seen for the proteomic results except the “coenzyme transport and metabolism” group was additionally over represented. In methanol-grown cells, the three functional categories significantly elevated in expression relative to acetate-grown cells were “amino acid transport and metabolism”, “coenzyme transport and metabolism”, and “translation”. A similar COG group pattern was seen for the proteomic results except the “nucleotide transport and metabolism” and “replication, recombination and repair” groups were additionally over represented. Therefore, translation machinery demand appears elevated due to methanol dependent cell growth similar to that reported for *M. mazei*[11] and consistent with the faster growth rate for these species on methanol compared to acetate [9-11].

Methanol conversion to methane

A total of 184 proteins were more abundant, and the expression of 210 genes up regulated, (Table 2) in methanol-grown *M. acetivorans*. Transcriptional profiling of *M. mazei* identified 212 genes at least 2.5-fold up regulated in response to growth on methanol [11], many of which encode proteins specific to the previously well-characterized pathway of methanol conversion to methane in *Methanosarcina* species [11, 45, 46]. The proteomic and microarray analyses of methanol- *vs.* acetate-grown *M. acetivorans* (Tables 1 and S1) indicated that the pathway for conversion of methanol to methane is similar to all other *Methanosarcina* species investigated. Many of the transcripts and proteins found to be greater in methanol- vs. acetate-grown *M. acetivorans* are involved in translation and biosynthesis (Table S1), consistent with the transcriptional profile of *M. mazei*[11]. Both *M. mazei*[11] and *M. acetivorans*[31] have doubling times for growth on methanol that are 4-5 times greater than that for acetate, and it has been

NIH-PA Author Manuscript

NIH-PA Author Manuscript

NIH-PA Author Manuscript

proposed [11] that the faster growth rate with methanol requires elevated levels of the translational apparatus and biosynthetic enzymes.

The genome of *M. acetivorans* is predicted to encode three two-subunit methyltransferase isozymes specific for methanogenesis from methanol, two of which (MA0455-0456 and MA4391-4392) were more abundant in methanol-grown cells, and the third (MA1616-1617) more abundant in acetate-grown cells (Table 1). Recent reporter gene studies of *M. acetivorans* are consistent with these results [47], and analogous to increased expression of genes in acetate- *vs.* methanol-grown *M. mazei*[11] encoding one of three methanol-specific methyltransferase isozymes. It has been reported that individual disruption of genes encoding the three methyltransferase isozymes had no effect on acetate-dependent growth of *M. acetivorans*, indicating none of the isozymes are essential for growth on acetate [27]. All of the above results are in agreement with a report where it was proposed that one of three methyltransferase isozymes synthesized in acetate-grown *Methanosarcina thermophila* facilitates transition from growth on acetate to growth on methanol [13].

Several group I chaperonins (MA1477, MA1479 and MA4413), and transcripts of genes encoding group I chaperonins (MA0630 and MA4413), were elevated in methanol-grown *M. acetivorans* (Table 1). MA0630 encodes GroEL that is clustered with MA0631 encoding GroES (Fig. 2) consistent with co-transcription and the coordinated roles for folding proteins described for species from the Bacteria domain. MA1477 and MA1479 encode GrpE and DnaJ, and are clustered with MA1478 encoding DnaK (Fig. 2) consistent with co-transcription and function in the Hsp70 system shown to assist protein folding in species from the Bacteria domain. The results confirm a previous report that MA1477 is up regulated in methanol-grown *M. acetivorans*, consistent with the reported up regulation of genes encoding the Hsp70 system in heat-shocked *M. mazei*[48-50] and *Methanococcoides burtonii* grown at high temperature [4]. A role for the group I chaperonins in *M. acetivorans* grown on methanol *vs.* acetate is less obvious, although it was previously proposed that the higher growth rate on methanol requires chaperonins to meet the increased demand for protein synthesis [10].

Thus, it appears there are few differences between growth on methanol between *M. acetivorans* and *M. mazei*, with one notable exception. A gene annotated to encode a flavodoxin (MA2699) was expressed 29-fold greater in methanol- *vs.* acetate-grown *M. acetivorans* (Table 1), consistent with an electron transport function during growth on methanol. The only gene (MM0261) in the genome of *M. mazei* with sequence identity to MA2699 encodes a putative flavoprotein with only 26% identity to the flavodoxin encoded by MA2699 [11]. These results suggest that the *M. acetivorans* flavodoxin (MA2699) does not have a functional equivalent in *M. mazei* and may reflect differences in electron transport between these marine and freshwater species.

Conversion of acetate to methane

Proteomic analyses identified 71 proteins that were more abundant in acetate-grown *M. acetivorans*, and microarray analyses identified a greater expression of 200 genes in acetate-grown cells (Tables 1 and S1). These results are similar to the number of genes reported to be up regulated in acetate- *vs.* methanol-grown *M. mazei*[11].

The CO dehydrogenase/acetyl-CoA synthase (Cdh) is central to the pathway for conversion of acetate to methane in freshwater *Methanosarcina* species and *M. acetivorans*[30, 51] where it cleaves acetyl-CoA releasing the methyl group for eventual reduction to methane and oxidizing the carbonyl group to carbon dioxide with transfer of electrons to ferredoxin. The genome of *M. acetivorans* is annotated with duplicate gene clusters (MA1011-1016 and MA3860-3865), each encoding the five subunits of the Cdh complex (CdhABCDE). The amino acid sequences of each cluster share greater than 90% identity [52]. A remarkable feature of the

NIH-PA Author Manuscript

NIH-PA Author Manuscript

NIH-PA Author Manuscript

genomic sequences of *M. mazei* and *M. acetivorans* is the extensive gene redundancy which has raised questions regarding the expression and physiological significance of duplicated genes [22, 53]. The genome of *M. mazei* also contains >90% identical duplicate gene clusters encoding the Cdh complex; however, transcriptional profiling was unable to distinguish the level of expression between clusters with strict confidence due to the high sequence identity and potential cross hybridization [11]. This same limitation applies to the DNA microarray results for *M. acetivorans* reported here, although data for MA1014, MA1016, MA3863, and MA3865 were in agreement with the proteomic results (Table 1) indicating up regulation of both operons in acetate- *vs.* methanol-grown cells. The three subunits encoded by MA3860-3862 and MA1014-1016 (Table 1) were in substantially greater abundance in acetate-grown *vs.* methanol grown cells (Table 1). Each of the six proteins was identified by high confidence MS/MS peptide sequencing of at least three unique peptide pairs. Co-transcription of all the genes in each cluster from *M. acetivorans* is supported by arrangement in the genome [52] (Fig. 2) which is identical to the operon characterized for *M. thermophila*[54]. These results strongly indicate that both Cdh complexes function in acetate-grown cells. The microarray results show MA4399, encoding the CdhA subunit of the Cdh complex, is up regulated in acetate-grown cells suggesting a role for this additional CdhA subunit in the conversion of acetate to methane. However, MA4399 is remote from the two complete *cdh* operons and not clustered with genes encoding the other four subunits of the complex; thus, the role for this additional CdhA subunit is not immediately apparent. Finally, these results further demonstrate how the combination of proteomic and microarray approaches extends the information beyond that achievable by either approach alone.

A previous report [30] described a co-transcribed gene cluster (MA0658-0665) in *M. acetivorans* proposed to encode an eight-subunit membrane-bound complex (Ma-Rnf). The report also showed three of the subunits are in greater abundance for acetate- *vs.* methanol-grown *M. acetivorans*[30]. The microarray analysis reported here showed four of the genes were up regulated in acetate-grown cells (Table 1) consistent with the previously reported proteomic analyses [30]. The proposed function for Ma-Rnf is to transfer electrons from reduced ferredoxin to methanophenazine generating a Na^+ gradient (high outside) (Fig. 3A). This electron transport chain is distinct from that proposed for freshwater *Methanosarcina* species [55-57] (Fig. 3B) for which the Ech hydrogenase oxidizes ferredoxin producing H_2 that is oxidized by the Vho hydrogenase generating a H^+ gradient (high outside). Transcriptional profiling (Table 1) also showed greater expression of genes (MA4566-4570 and MA4572) in acetate *vs.* methanol-grown *M. acetivorans* previously shown to be co-transcribed with genes (MA4566-4572) annotated to encode a seven-subunit Na^+/H^+ antiporter (Ma-Mrp). The relative levels of the transcripts were consistent with the previously reported proteomic analyses [30] for which two of the gene products (MA4567 and MA4568) were in greater abundance in acetate-grown cells. The antiporter is proposed to function during growth on acetate by exchanging the Ma-Rnf-generated Na^+ gradient (Fig. 3A) for a H^+ gradient that drives ATP synthesis [30].

A role for flavodoxins in the pathway of acetate conversion to methane has not been reported for any methanogenic species. Microarray analysis (Table 1) identified a flavodoxin gene (MA1799) up regulated 3-fold in acetate-grown *M. acetivorans*. This flavodoxin has only 26% identity to the flavodoxin encoded by MA2699 that is expressed 29-fold greater in methanol-grown cells (Table 1), consistent with different electron transport functions for each flavodoxin that are specific for growth with the respective substrates. The only flavodoxin encoded in the *M. mazei* genome (MM0261) with identity to MA1799 (27%) was not reported among differentially expressed genes [11]. The only other flavodoxin gene (MM0637) reported up regulated in acetate- *vs.* methanol-grown *M. mazei* has no homologs in the genome of *M. acetivorans*[52]. These results suggest different flavodoxins function in acetate-grown *M.*

NIH-PA Author Manuscript

NIH-PA Author Manuscript

NIH-PA Author Manuscript

acetivorans and *M. mazei* that further distinguishes electron transport in marine *vs.* freshwater *Methanosarcina* species.

A polyferredoxin, and expression of the encoding gene (MA2867), was greater in acetate- *vs.* methanol-grown cells (Table 1) consistent with a role in electron transport during growth with acetate. MA2867 is clustered with MA2868 (Fig. 2), the product of which was in greater abundance in acetate-grown cells. Interestingly, MA2868 is a fusion of *hdrA* and *mvhD*. HdrA is a subunit of the HdrABC-type of heterodisulfide reductase that functions to reduce CoM-S-S-CoB in the pathway for reduction of CO_2 to methane with H_2 as the electron donor. HdrA is the entry point for transfer of electrons to the HdrBC subunits harboring the site for reduction of the heterodisulfide [58, 59]. MvhD is a subunit of the Mvh hydrogenase that functions in H_2-utilizing CO_2-reducing species other than *Methanosarcina*[52]. It is proposed that the MvhD subunit mediates electron transfer to the HdrA subunit of the HdrABC-type of heterodisulfide reductase [59]. These results are consistent with an electron transport role for the putative HdrA::MvhD fusion protein during growth on acetate. However, *M. acetivorans* is unable to reduce CO_2 to methane with H_2, and the HdrDE-type of heterodisulfide reductase (Fig. 3A) is postulated to function during growth on acetate [30]. Thus, a role for the HdrABC-type during growth on acetate is unlikely and raises the question of a role for the putative HdrA::MvhD fusion protein during growth on acetate.

Iron-sulfur flavoprotein (Isf) was previously hypothesized to function in the electron transport scheme of acetate-grown *M. thermophila*[60], and more recently for *M. mazei*[11]. Remarkably, the genome of *M. acetivorans* is annotated with nineteen *isf* homologs [52] for which microarray analysis showed two (MA2167 and MA0406) were up regulated in acetate- *vs.* methanol-grown cells (Table 1). This result is consistent with *M. mazei* based on the up regulation in acetate-grown cells of an *isf* homolog [11], among eleven *isf* homologs, in the genome of *M. mazei*[52]. The recent crystal structures of Isf from *M. thermophila* and *Archaeoglobus fulgidus* shows similarity to rubredoxin:oxygen oxidoreductase, an enzyme proposed to function in oxidative stress by reducing O_2 to water [61]. Indeed, the prototypic Isf from *M. thermophila* reduces O_2 and H_2O_2 to water [62]. Thus, it is possible Isf paralogs function in the oxidative stress response rather than an electron transport function in the acetate pathway.

The protein product of MA3972 was in greater abundance, and expression of the gene up regulated in acetate-grown cells (Table 1). Although MA3972 is annotated as a conserved hypothetical protein with a molecular mass of 59 kDa [52], the sequence is 90% identical to MM0940 of *M. mazei* encoding a 59-kDa putative flavoprotein of unknown function that is also up regulated in acetate-grown cells [11]. The results suggest that the product of MM0940 and MA3972 is a core flavoprotein with an unknown function in the acetate pathways of freshwater and marine *Methanosarcina* species.

Stress—The previously reported 2-D gel proteomic analysis of *M. acetivorans* identified a peroxiredoxin (MA4103) that was in greater amounts in acetate- *vs.* methanol-grown cells [10]. Peroxiredoxins reduce H_2O_2 to water in response to oxidative stress. The microarray results reported here identified seven additional genes, with potential to respond to oxidative stress, that were up regulated in acetate-grown cells (Table 1 and Fig. 4). MA4103 encodes a peroxiredoxin, and MA0406 and MA2167 encode paralogs of the Isf family for which the prototype reduces O_2 and H_2O_2 to water [62]. MA3743 is annotated to encode flavoprotein A which reduces O_2 to water in *Methanobrevibacter arboriphilus*[63]. MA3212 is annotated as thioredoxin, a family of proteins acting as general disulfide reductases in the oxidative stress response. In contrast, methanol-grown cells showed no elevated expression of genes or elevated abundance of proteins involved in the oxidative stress response. Further, MA1189 is annotated to encode a tryptophan repressor binding protein (WrbA) previously proposed to be a regulatory protein in *Escherichia coli*; however, it was recently shown that WrbA from *E.*

NIH-PA Author Manuscript

NIH-PA Author Manuscript

NIH-PA Author Manuscript

coli is the prototype of a new family of NAD(P)H:quinone oxidoreductases implicated in the oxidative stress response of procaryotes from both the Bacteria and Archaea domains [64]. Nonetheless, a regulatory role in the stress response cannot be ruled out at this juncture. Overall, these results indicate that an oxidative stress response is induced in acetate-grown *vs.* methanol-grown *M. acetivorans*. Cells cultured with either substrate were grown under strict anaerobic conditions with the same amounts of reducing agent. One possible explanation for the oxidative stress response in acetate-grown cells is the long doubling time (84 h) compared to methanol-grown cells (42 h) which induced a general stress response that includes oxidative stress. Genes encoding other stress-related proteins (MA0133, MA1682, MA3284, MA4542) were also expressed greater in acetate- *vs.* methanol-grown cells (Table 1).

Proteomic and microarray approaches also identified a suite of genes that function in polyphosphate (polyP) formation for which the protein products were more abundant or expression of the genes were greater in acetate-grown cells (Table 1, Fig. 4). The gene cluster MA0081-0083 (Fig. 2) encodes for polyphosphate kinase (MA0081) and exopolyphosphatase (MA0083), both of which have been characterized from the Bacteria domain [65]. The former catalyzes the synthesis of polyP from the gamma phosphate of ATP, and the latter cleaves inorganic phosphate from polyP in a processive manner to maintain homeostasis of polyP levels. Both enzymes in *Escherichia coli* are encoded on an operon [66] reminiscent of the MA0081-0083 gene cluster in *M. acetivorans* except for an intervening gene (MA0082) of unknown function (Fig. 2). Microarray analysis showed expression of a gene encoding a second exopolyphosphatase (MA2351) was also up regulated in acetate-grown cells (Table 1). Also, either the protein product or gene expression increased in response to acetate for three genes (MA0887, MA0889 and MA0891) of a five-gene cluster (MA0887-0891) (Fig. 2) encoding proteins of the Pst phosphate transport system described in species from the Bacteria domain [67]. Overall, these results are consistent with greater expression of genes in acetate-grown cells of *M. acetivorans* that function in polyP formation. The organization of genes encoding the Pst system (Fig. 2) is identical to that in *E. coli* which includes a gene encoding the regulatory protein PhoU (MA0891). In the Bacteria domain, PhoU is part of the phosphate regulon which functions to assimilate phosphate wherein PhoU is a negative effector of the response regulator in a two-component regulatory system [67]. The results are consistent with a role for the product of MA0891 in the regulation of phosphate uptake by one of several uncharacterized two-component systems in *M. acetivorans* discussed in the next section.

A role has been proposed for polyP in response to a variety of stressors, including oxidative stress, for members of the Bacteria domain [65, 68, 69]. In the Bacteria, *ppk*$^-$ mutants lacking polyP fail to express *rpoS* encoding a regulatory sigma factor that governs the expression of genes essential to resist a variety of stress conditions during stationary phase [70]. Thus, enzymes required for polyP synthesis in acetate-grown cells of *M. acetivorans* is consistent with a role in the general stress response. Although a specific function has yet to be determined, it is interesting to note that polyphosphate kinase is necessary to protect *Salmonella enterica* from stress imposed by growth in the presence of acetic acid [71]. It is proposed that polyphosphate acts as a chemical chaperonin, helping to refold proteins denatured by acetic acid and oxidative stress.

Regulation—The genome of *M. acetivorans* is annotated with an unusually large number (fifty) of sensory transduction histidine kinase proteins and a considerably smaller number (eighteen) of cognate proteins with response regulator receiver domains [22]. Further, only one of the proteins with a receiver domain is of sufficient length to also harbor an effector domain. These anomalies compared to the two-component regulatory systems in the Bacteria domain raise questions regarding the expression and roles for the putative sensory and response proteins of *M. acetivorans*. The results indicate that fifteen genes encoding sensory proteins were expressed in *M. acetivorans* (not shown) of which nine were differentially expressed between

NIH-PA Author Manuscript

NIH-PA Author Manuscript

NIH-PA Author Manuscript

methanol- and acetate-grown cells (Table 1), a result suggesting possible roles for these proteins during growth on acetate or methanol. Furthermore, genes encoding five proteins with receiver domains were expressed (not shown) for which two were differentially expressed (Table 1).

More energy is available when converting methanol ($\Delta G^{\circ\prime}$ = -106.5 kJ) *vs.* acetate ($\Delta G^{\circ\prime}$ = -36 kJ) to methane; thus, *Methanosarcina* species regulate genes specific for each substrate with a preference for methanol [45]. However, little is understood regarding the mechanism of gene regulation in response to the growth substrate. Several regulatory proteins were in greater abundance (MA0368, MA1763, and MA2914), and expression of genes encoding regulatory proteins up regulated (MA0924, MA1122, MA1487, MA2914, and MA3916) in methanol-grown *M. acetivorans* (Table 1). The results suggest roles for these proteins in regulating the expression of genes specific to the growth substrate. MA0368 and MA1487 encode TetR family regulatory proteins, and the genome of *M. acetivorans* is annotated with an additional eleven genes encoding TetR family proteins [52] suggesting a role in regulation. MA1487 is clustered with MA1486, annotated as a MoaA/NifB family protein, that is also expressed greater in methanol- *vs.* acetate-grown cells. MoaA functions in the synthesis of molybdopterin, a cofactor of the formyl-methanofuran dehydrogenase (MA0304-0309) which functions in the pathway of methanol conversion to methane and is in greater abundance in methanol-grown cells (Table 1). MoaB (MA0187), also involved in molybdopterin biosynthesis, was also in greater abundance in methanol-grown cells. The MarR family regulatory protein encoded by MA1122 has 76% identity to MarR encoded by MM3195 in *M. mazei* that is also expressed greater in methanol- *vs.* acetate-grown cells of *M. mazei*[11]. All other genes encoding regulatory proteins expressed in *M. acetivorans* were not among the genes reported to be differentially expressed in *M. mazei*[11].

Microarray analysis showed MA3916 encoding the GlnK regulatory protein was up regulated in methanol-grown cells (Table 1) and previously shown to be a regulator of ammonium assimilation in *M. mazei*[72]. MA3916 is clustered with MA3917 and MA3918 (Fig. 2), both encoding ammonium transporters, also up regulated in methanol-grown cells (Table 1), consistent with the regulatory function of GlnK. The apparent requirement for increased ammonium in methanol- *vs.* acetate-grown cells could reflect the greater growth rate in methanol-grown cells and an increased need for nutrients.

Conclusions—A combination of advanced proteomics and DNA microarray analyses of *M. acetivorans*, the first for any methanosarcina species, has extended the physiological understanding for growth and methanogenesis with either acetate or methanol as substrates. The two experimental approaches were in good agreement, and the different capabilities were highly complementary leading to discovery not possible by each method alone. The proteomic results indicated that duplicate CO dehydrogenase/acetyl-CoA complexes function in the conversion of acetate to methane, a question not resolvable by microarray analysis alone. The gene expression ratios for stress-related proteins were greater in acetate- *versus* methanol-grown cells supporting an earlier proteomic study suggesting that a general stress response is elicited by growth on acetate. Novel roles were suggested for electron transport proteins specific for either growth substrate. The results also identified several regulatory proteins, commonly found in the Bacteria domain, suggested to function during growth of *M. acetivorans* with acetate or methanol. Finally, the results also suggested roles for two-component regulatory systems specific for each growth substrate.

Supplementary Material

Refer to Web version on PubMed Central for supplementary material.

NIH-PA Author Manuscript

NIH-PA Author Manuscript

NIH-PA Author Manuscript

Acknowledgements

This work was supported by NSF grant MCB-0110762 to J.G.F., NIH grant GM15847 to B.L.K, and a Department of Energy Biosciences Division grant award DE-FG03-86ER13498 to R.P.G. Contribution number 886 from the Barnett Institute.

References

1. Zinder, S. Physiological ecology of methanogens. In: Ferry, JG., editor. Methanogenesis. Chapman and Hall; New York, NY: 1993. p. 128-206.
2. McCarty PL. The development of anaerobic treatment and its future. Water Sci Technol 2001;44(8): 149–56. [PubMed: 11730130]
3. Ferry, JG. One-carbon metabolism in methanogenic anaerobes. In: Ljungdahl, LG.; Adams, MW.; Barton, LL.; Ferry, JG.; Johnson, MK., editors. Biochemistry and Physiology of Anaerobic Bacteria. Springer-Verlag; New York: 2003. p. 143-156.
4. Goodchild A, Saunders NFW, Ertan H, Raftery M, Guilhaus M, Curmi PMG, Cavicchioli R. A proteomic determination of cold adaptation in the antarctic archaeon, *Methanococcoides burtonii*. Mol Microbiol 2004;53:309–321. [PubMed: 15225324]
5. Goodchild A, Raferty M, Saunders NFW, Guilhaus M, Cavicchioli R. Biology of the cold-adapted archaeon, *Methanococcoides burtonii*, determined by proteomics using liquid chromatography-tandem mass spectrometry. J Proteome Res 2004;3:1164–1176. [PubMed: 15595725]
6. Saunders NFW, Goodchild A, Raftery M, Guilhaus M, Curmi PMG, Cavicchioli R. Predicted roles for hypothetical proteins in the low-temperature expressed proteome of the antarctic archaeon *Methanococcoides burtonii*. J Proteome Res 2005;4:464–472. [PubMed: 15822923]
7. Goodchild A, Raftery M, Saunders NFW, Guilhaus M, Cavicchioli R. Cold adaptation of the antarctic archaeon, *Methanococcoides burtonii*, assessed by proteomics using ICAT. J Proteome Res 2005;4:473–480. [PubMed: 15822924]
8. Nichols DS, Miller MR, Davies NW, Goodchild A, Raftery M, Cavicchioli R. Cold adaptation in the antarctic archaeon *Methanococcoides burtonii* involves membrane lipid unsaturation. J Bacteriol 2004;186(24):8508–8515. [PubMed: 15576801]
9. Li Q, Li L, Rejtar T, Karger BL, Ferry JG. The proteome of *Methanosarcina acetivorans*. Part I, an expanded view of the biology of the cell. J Proteome Res 2005;4:112–128. [PubMed: 15707366]
10. Li Q, Li L, Rejtar T, Karger BL, Ferry JG. The proteome of *Methanosarcina acetivorans*. Part II, comparison of protein levels in acetate- and methanol-grown cells. J Proteome Res 2005;4:129–136. [PubMed: 15707367]
11. Hovey R, Lentes S, Ehrenreich A, Salmon K, Saba K, Gottschalk G, Gunsalus RP, Deppenmeier U. DNA microarray analysis of *Methanosarcina mazei* Go1 reveals adaptation to different methanogenic substrates. Mol Genet Genomics 2005;273:225–239. [PubMed: 15902489]
12. Veit K, Ehlers C, Ehrenreich A, Salmon K, Hovey R, Gunsalus RP, Deppenmeier U, Schmitz RA. Global transcriptional analysis of *Methanosarcina mazei* strain Go1 under different nitrogen availabilities. Mol Genet Genomics. 2006
13. Ding YH, Zhang SP, Tomb JF, Ferry JG. Genomic and proteomic analyses reveal multiple homologs of genes encoding enzymes of the methanol:coenzyme M methyltransferase system that are differentially expressed in methanol- and acetate-grown *Methanosarcina thermophila*. FEMS Microbiol Lett 2002;215(1):127–132. [PubMed: 12393212]
14. Farhoud MH, Wessels HJ, Steenbakkers PJ, Mattijssen S, Wevers RA, van Engelen BG, Jetten MS, Smeitink JA, van den Heuvel LP, Keltjens JT. Protein complexes in the archaeon *Methanothermobacter thermautotrophicus* analyzed by Blue Native/SDS-PAGE and mass spectrometry. Mol Cell Proteomics 2005;4(11):1653–63. [PubMed: 16037073]
15. Zhu W, Reich CI, Olsen GJ, Giometti CS, Yates JR 3rd. Shotgun proteomics of *Methanococcus jannaschii* and insights into methanogenesis. J Proteome Res 2004;3(3):538–48. [PubMed: 15253435]
16. Giometti CS, Reich C, Tollaksen S, Babnigg G, Lim H, Zhu W, Yates J, Olsen G. Global analysis of a “simple” proteome: *Methanococcus jannaschii*. J Chromatogr B Analyt Technol Biomed Life Sci 2002;782(12):227–43.

NIH-PA Author Manuscript NIH-PA Author Manuscript NIH-PA Author Manuscript

17. Porat I, Kim W, Hendrickson EL, Xia Q, Zhang Y, Wang T, Taub F, Moore BC, Anderson IJ, Hackett M, Leigh JA, Whitman WB. Disruption of the operon encoding Ehb hydrogenase limits anabolic CO_2 assimilation in the archaeon *Methanococcus maripaludis*. J Bacteriol 2006;188(4):1373–1380. [PubMed: 16452419]

18. Xia Q, Hendrickson EL, Zhang Y, Wang T, Taub F, Moore BC, Porat I, Whitman WB, Hackett M, Leigh JA. Quantitative proteomics of the archaeon *Methanococcus maripaludis* validated by microarray analysis and real time PCR. Mol Cell Proteomics 2006;5(5):868–881. [PubMed: 16489187]

19. Forbes AJ, Patrie SM, Taylor GK, Kim YB, Jiang L, Kelleher NL. Targeted analysis and discovery of posttranslational modifications in proteins from methanogenic Archaea by top-down MS. Proc Natl Acad Sci U S A 2004;101:2678–2683. [PubMed: 14976258]

20. Mukhopadhyay B, Johnson EF, Wolfe RS. A novel pH_2 control on the expression of flagella in the hyperthermophilic strictly hydrogenotrophic methanarchaeaon *Methanococcus jannaschii*. Proc Natl Acad Sci U S A 2000;97(21):11522–11527. [PubMed: 11027352]

21. Giometti CS, Reich CI, Tollaksen SL, Babnigg G, Lim H, Yates JR, Olsen GJ. Structural modifications of *Methanococcus jannaschii* flagellin proteins revealed by proteome analysis. Proteomics 2001;1:1033–1042. [PubMed: 11683504]

22. Galagan JE, Nusbaum C, Roy A, Endrizzi MG, Macdonald P, FitzHugh W, Calvo S, Engels R, Smirnov S, Atnoor D, Brown A, Allen N, Naylor J, Stange-Thomann N, DeArellano K, Johnson R, Linton L, McEwan P, McKernan K, Talamas J, Tirrell A, Ye W, Zimmer A, Barber RD, Cann I, Graham DE, Grahame DA, Guss AM, Hedderich R, Ingram-Smith C, Kuettner HC, Krzycki JA, Leigh JA, Li W, Liu J, Mukhopadhyay B, Reeve JN, Smith K, Springer TA, Umayam LA, White O, White RH, de Macario EC, Ferry JG, Jarrell KF, Jing H, Macario AJ, Paulsen I, Pritchett M, Sowers KR, Swanson RV, Zinder SH, Lander E, Metcalf WW, Birren B. The genome of *M. acetivorans* reveals extensive metabolic and physiological diversity. Genome Res 2002;12(4):532–42. [PubMed: 11932238]

23. Metcalf WW, Zhang JK, Apolinario E, Sowers KR, Wolfe RS. A genetic system for Archaea of the genus *Methanosarcina*. Liposome-mediated transformation and construction of shuttle vectors. Proc Natl Acad Sci USA 1997;94:2626–2631. [PubMed: 9122246]

24. Zhang JK, Pritchett MA, Lampe DJ, Roberton HM, Metcalf WW. *In vivo* transposon mutagenesis of the methanogenic archaeon *Methanosarcina acetivorans* C2A using a modified version of the insect mariner-family transposable element Himar1. Proc Natl Acad Sci 2000;97(17):9665–9670. [PubMed: 10920201]

25. Zhang JK, White AK, Kuettner HC, Boccazzi P, Metcalf WW. Directed mutagenesis and plasmid-based complementation in the methanogenic archaeon *Methanosarcina acetivorans* C2A demonstrated by genetic analysis of proline biosynthesis. J Bacteriol 2002;184(5):1449–1454. [PubMed: 11844777]

26. Pritchett MA, Zhang JK, Metcalf WW. Development of a markerless genetic exchange method for *Methanosarcina acetivorans* C2A and its use in construction of new genetic tools for methanogenic archaea. Appl Environ Microbiol 2004;70(3):1425–1433. [PubMed: 15006762]

27. Pritchett MA, Metcalf WW. Genetic, physiological and biochemical characterization of multiple methanol methyltransferase isozymes in *Methanosarcina acetivorans* C2A. Mol Microbiol 2005;56 (5):1183–94. [PubMed: 15882413]

28. Rother M, Boccazzi P, Bose A, Pritchett MA, Metcalf WW. Methanol-dependent gene expression demonstrates that methyl-coenzyme M reductase is essential in *Methanosarcina acetivorans* C2A and allows isolation of mutants with defects in regulation of the methanol utilization pathway. J Bacteriol 2005;187(16):5552–5559. [PubMed: 16077099]

29. Mahapatra A, Patel A, Soares JA, Larue RC, Zhang JK, Metcalf WW, Krzycki JA. Characterization of a *Methanosarcina acetivorans* mutant unable to translate UAG as pyrrolysine. Mol Microbiol 2006;59(1):56–66. [PubMed: 16359318]

30. Li Q, Li L, Rejtar T, Lessner DJ, Karger BL, Ferry JG. Electron transport in the pathway of acetate conversion to methane in the marine archaeon *Methanosarcina acetivorans*. J Bacteriol 2006;188:702–710. [PubMed: 16385060]

31. Li Q, Li l, Rejtar T, Karger BL, Ferry JG. The proteome of *Methanosarcina acetivorans*. Part I, an expanded view of the biology of the cell. J Proteome Res 2004;4:112–128. [PubMed: 15707366]

NIH-PA Author Manuscript

NIH-PA Author Manuscript

NIH-PA Author Manuscript

32. Wolfe, RS.; Higgins, IJ. Microbial biochemistry of methane: a study in contrasts. University Park Press; Baltimore: 1979.
33. Nesterenko MV, Tilley M, Upton SJ. A simple modification of Blum's silver stain method allows for 30 minute detection of proteins in polyacrylamide gels. J Biochem Biophys Methods 1994;28:239–242. [PubMed: 8064118]
34. Shevchenko A, Wilm M, Vorm O, Mann M. Mass spectrometric sequencing of proteins silver-stained polyacrylamide gels. Anal Chem 1996;68:850–858. [PubMed: 8779443]
35. Washburn MP, Ulaszek R, Deciu C, Schieltz DM, Yates JR 3rd. Analysis of quantitative proteomic data generated via multidimensional protein identification technology. Anal Chem 2002;74:1650–1657. [PubMed: 12043600]
36. Andreev VP, Li L, Rejtar T, Li Q, Ferry JG, Karger BL. New algorithm for $^{15}N/^{14}N$ quantitation with LC-ESI-MS using an LTQ-FT mass spectrometer. J Proteome Res 2006;5:2039–2045. [PubMed: 16889428]
37. Nesvizhskii AI, Keller A, Kolker E, Aebersold R. A statistical model for identifying proteins by tandem mass spectrometry. Anal Chem 2003;75:4646–4658. [PubMed: 14632076]
38. Rohlin L, Trent JD, Salmon K, Kim U, Gunsalus RP, Liao JC. Heat shock response of *Archaeoglobus fulgidus*. J Bacteriol 2005;187(17):6046–6057. [PubMed: 16109946]
39. Pruss BM, Campbell JW, Van Dyk TK, Zhu C, Kogan Y, Matsumura P. FlhD/FlhC is a regulator of anaerobic respiration and the Entner-Doudoroff pathway through induction of the methyl-accepting chemotaxis protein Aer. J Bacteriol 2003;185(2):534–43. [PubMed: 12511500]
40. Hyduke DR, Rohlin L, Kao KC, Liao JC. A software package for cDNA microarray data normalization and assessing confidence intervals. Omics 2003;7(3):227–34. [PubMed: 14583113]
41. Tseng GC, Oh MK, Rohlin L, Liao JC, Wong WH. Issues in cDNA microarray analysis: quality filtering, channel normalization, models of variations and assessment of gene effects. Nucleic Acids Res 2001;29(12):2549–57. [PubMed: 11410663]
42. Oh MK, Rohlin L, Kao KC, Liao JC. Global expression profiling of acetate-grown *Escherichia coli*. J Biol Chem 2002;277(15):13175–13183. [PubMed: 11815613]
43. Li Q, Li L, Rejtar T, Karger BL, Ferry JG. The proteome of *Methanosarcina acetivorans*. Part II, comparison of protein levels in acetate- and methanol-grown cells. J Proteome Res 2004;4:129–136. [PubMed: 15707367]
44. Julka S, Regnier F. Quantification in proteomics through stable isotope coding: a review. J Proteome Res 2004;3(3):350–63. [PubMed: 15253416]
45. Jablonski PE, DiMarco AA, Bobik TA, Cabell MC, Ferry JG. Protein content and enzyme activities in methanol- and acetate-grown *Methanosarcina thermophila*. J Bacteriol 1990;172:1271–1275. [PubMed: 2307649]
46. Deppenmeier U. The unique biochemistry of methanogenesis. Prog Nucleic Acid Res Mol Biol 2002;71:223–283. [PubMed: 12102556]
47. Bose A, Pritchett MA, Rother M, Metcalf WW. Differential regulation of the three methanol methyltransferase Isozymes in *Methanosarcina acetivorans* C2A. J Bacteriol 2006;188(20):7274–7283. [PubMed: 17015666]
48. Lange M, Tolker-Nielsen T, Molin S, Ahring BK. In situ reverse transcription-PCR for monitoring gene expression in individual *Methanosarcina mazei* S-6 cells. Appl Environ Microbiol 2000;66(5):1796–800. [PubMed: 10788341]
49. De Biase A, Macario AJL, de Macario EC. Effect of heat stress on promoter cytosol of the archae binding by transcription factors in the on Methanosarcina mazeii. Gene 2002;282(12):189–197. [PubMed: 11814691]
50. Conway De Macario E, Clarens M, Macario AJ. Archaeal *grpE*: transcription in two different morphologic stages of *Methanosarcina mazei* and comparison with *dnaK* and *dnaJ*. J Bacteriol 1995;177(3):544–550. [PubMed: 7836285]
51. Ferry JG. Enzymology of one-carbon metabolism in methanogenic pathways. FEMS Microbiol Rev 1999;23(1):13–38. [PubMed: 10077852]
52. http://www.tigr.org.
53. Deppenmeier U, Johann A, Hartsch T, Merkl R, Schmitz RA, Martinez-Arias R, Henne A, Wiezer A, Baumer S, Jacobi C, Bruggemann H, Lienard T, Christmann A, Bomeke M, Steckel S,

NIH-PA Author Manuscript

NIH-PA Author Manuscript

NIH-PA Author Manuscript

Bhattacharyya A, Lykidis A, Overbeek R, Klenk HP, Gunsalus RP, Fritz HJ, Gottschalk G. The genome of *Methanosarcina mazei*: evidence for lateral gene transfer between Bacteria and Archaea. J Mol Microbiol Biotechnol 2002;4(4):453–61. [PubMed: 12125824]

54. Maupin-Furlow JA, Ferry JG. Analysis of the CO dehydrogenase/acetyl-coenzyme A synthase operon of *Methanosarcina thermophila*. J Bacteriol 1996;178:6849–6856. [PubMed: 8955306]
55. Hedderich R. Energy-converting [NiFe] hydrogenases from Archaea and extremophiles: ancestors of complex I. J Bioenerg Biomembr 2004;36:65–75. [PubMed: 15168611]
56. Meuer J, Bartoschek S, Koch J, Kunkel A, Hedderich R. Purification and catalytic properties of Ech hydrogenase from *Methanosarcina barkeri*. Eur J Biochem 1999;265(1):325–335. [PubMed: 10491189]
57. Meuer J, Kuettner HC, Zhang JK, Hedderich R, Metcalf WW. Genetic analysis of the archaeon *Methanosarcina barkeri* Fusaro reveals a central role for Ech hydrogenase and ferredoxin in methanogenesis and carbon fixation. Proc Natl Acad Sci U S A 2002;99(8):5632–5637. [PubMed: 11929975]
58. Setzke E, Hedderich R, Heiden S, Thauer RK. H_2:heterodisulfide oxidoreductase complex from *Methanobacterium thermoautotrophicum*: composition and properties. Eur J Biochem 1994;220:139–148. [PubMed: 8119281]
59. Stojanowic A, Mander GJ, Duin EC, Hedderich R. Physiological role of the F_{420}-non-reducing hydrogenase (Mvh) from *Methanothermobacter marburgensis*. Arch Microbiol 2003;180(3):194–203. [PubMed: 12856108]
60. Latimer MT, Painter MH, Ferry JG. Characterization of an iron-sulfur flavoprotein from *Methanosarcina thermophila*. J Biol Chem 1996;271:24023–24028. [PubMed: 8798638]
61. Andrade SLA, Cruz F, Drennan CL, Ramakrishnan V, Rees DC, Ferry JG, Einsle O. Structures of the iron-sulfur flavoproteins from *Methanosarcina thermophila* and *Archaeoglobus fulgidus*. J Bacteriol 2005;187:3848–3854. [PubMed: 15901710]
62. Cruz FC, Ferry JG. Interaction of iron-sulfur flavoprotein with oxygen and hydrogen peroxide. Biochim Biophys Acta 2006;1760:858–864. [PubMed: 16624489]
63. Seedorf H, Dreisbach A, Hedderich R, Shima S, Thauer R. K, $F_{420}H_2$ oxidase (FprA) from *Methanobrevibacter arboriphilus*, a novel coenzyme F_{420} dependent enzyme involved in O_2 detoxification. Arch Microbiol 2004;182:126–137. [PubMed: 15340796]
64. Patridge EV, Ferry JG. WrbA from *Escherichia coli* and *Archaeoglobus fulgidus* is an NAD(P)H:quinone oxidoreductase. J Bacteriol 2006;188(10):3498–3506. [PubMed: 16672604]
65. Kornberg A, Rao NN, Ault-Riche D. Inorganic polyphosphate: a molecule of many functions. Annu Rev Biochem 1999;68:89–125. [PubMed: 10872445]
66. Akiyama M, Crooke E, Kornberg A. An exopolyphosphatase of *Escherichia coli*. The enzyme and its *ppx* gene in a polyphosphate operon. J Biol Chem 1993;268(1):633–9. [PubMed: 8380170]
67. van Veen HW. Phosphate transport in prokaryotes: molecules, mediators and mechanisms. Antonie Van Leeuwenhoek 1997;72(4):299–315. [PubMed: 9442271]
68. Crooke E, Akiyama M, Rao NN, Kornberg A. Genetically altered levels of inorganic polyphosphate in *Escherichia coli*. J Biol Chem 1994;269(9):6290–5. [PubMed: 8119977]
69. Rao NN, Kornberg A. Inorganic polyphosphate supports resistance and survival of stationary-phase *Escherichia coli*. J Bacteriol 1996;178(5):1394–400. [PubMed: 8631717]
70. Shiba T, Tsutsumi K, Yano H, Ihara Y, Kameda A, Tanaka K, Takahashi H, Munekata M, Rao NN, Kornberg A. Inorganic polyphosphate and the induction of *rpoS* expression. Proc Natl Acad Sci U S A 1997;94(21):11210–5. [PubMed: 9326588]
71. Price-Carter M, Fazzio TG, Vallbona EI, Roth JR. Polyphosphate kinase protects *Salmonella enterica* from weak organic acid stress. J Bacteriol 2005;187(9):3088–99. [PubMed: 15838036]
72. Ehlers C, Grabbe R, Veit K, Schmitz RA. Characterization of G1nK(1) from *Methanosarcina mazei* strain Go1: Complementation of an *Escherichia coli glnK* mutant strain by GlnK(1). J Bacteriol 2002;184(4):1028–1040. [PubMed: 11807063]

NIH-PA Author Manuscript

NIH-PA Author Manuscript

NIH-PA Author Manuscript

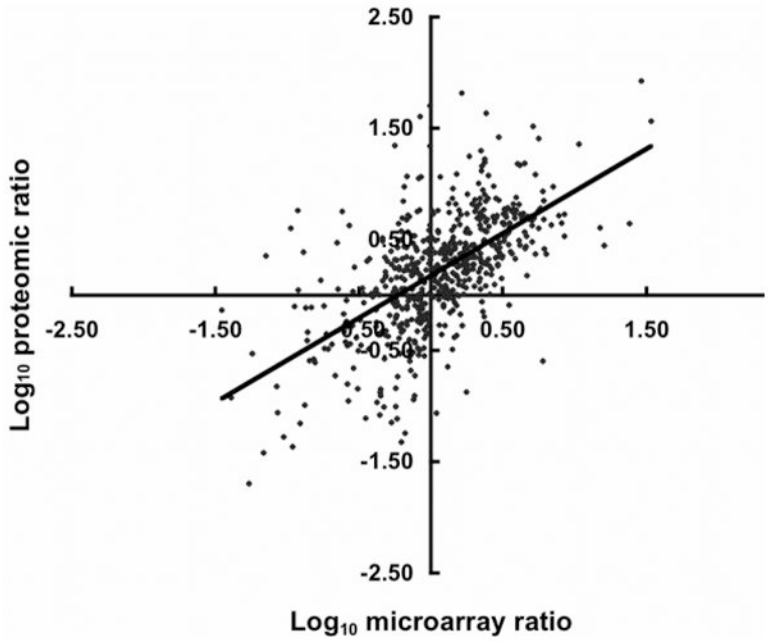

Figure 1.
The differential expression of selected ORFs for proteomic and microarray data. For each ORF, the log change for proteomic data is plotted on the X axis and the corresponding microarray data on the Y axis. Data are available in Tables 1 and S1.

NIH-PA Author Manuscript

NIH-PA Author Manuscript

NIH-PA Author Manuscript

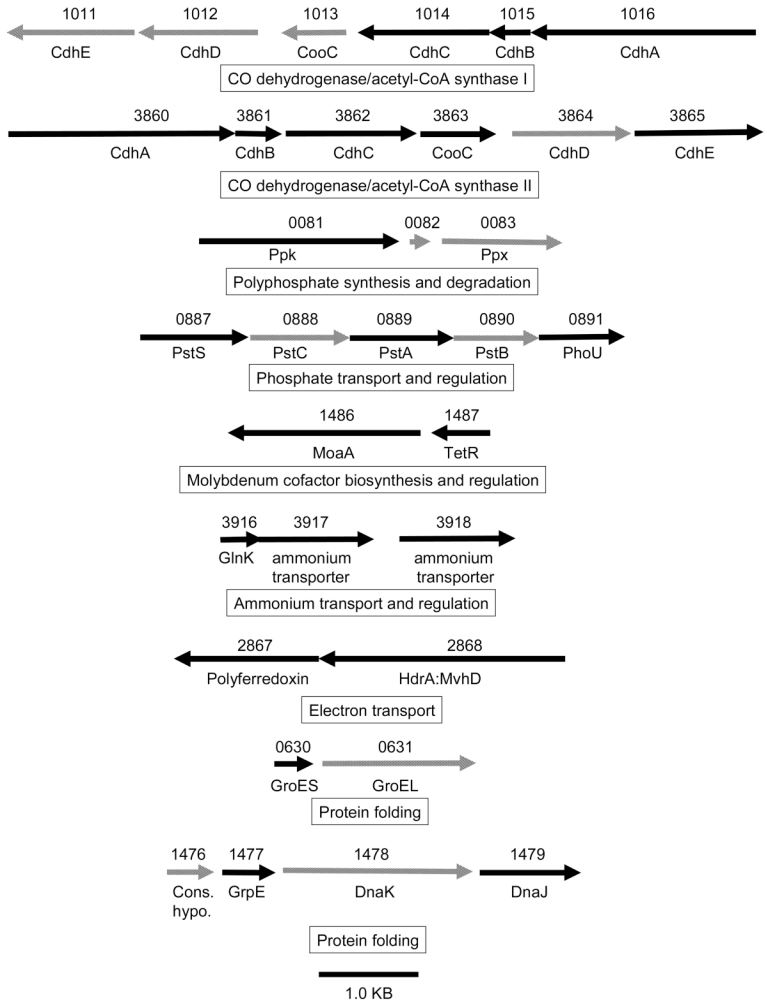

Figure 2.

Organization of differentially expressed genes and genes encoding differentially abundant proteins. Arrows indicate the length and orientation of genes. Hatched arrows indicate genes not represented in the proteome or transcriptome. The numbers above the arrows correspond to the gene loci. See Table 1 for gene annotations.

NIH-PA Author Manuscript

NIH-PA Author Manuscript

NIH-PA Author Manuscript

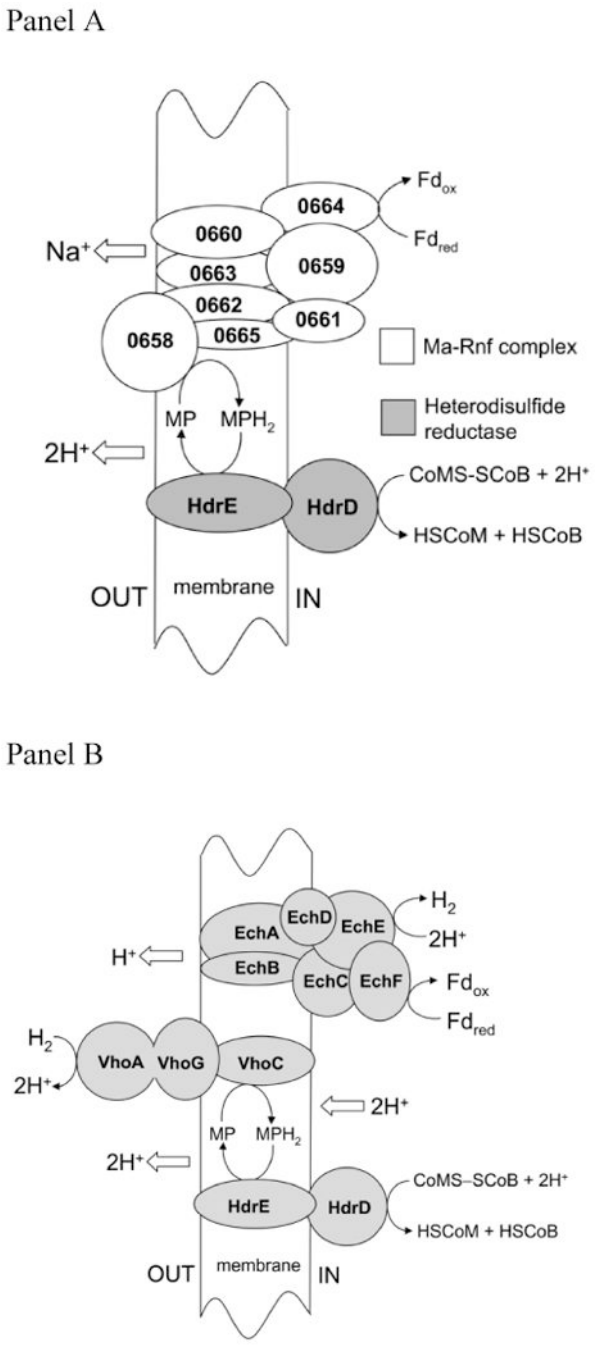

Figure 3.

Panel A. Electron transport proposed for acetate-grown *Methanosarcina acetivorans*. The numbers represent the loci of genes encoding subunits of Ma-Rnf. Fd, ferredoxin; MP, methanophenazine; CoM; coenzyme M, CoB; coenzyme B; HdrDE; heterodisulfide reductase. Panel B. Electron transport proposed for acetate-grown freshwater *Methanosarcina* species. EchA-F, subunits of the Ech hydrogenase; Fd, ferredoxin; VhoACG, subunits of the Vho hydrogenase; MP, methanophenazine; CoM; coenzyme M, CoB; coenzyme B; HdrDE; heterodisulfide reductase.

NIH-PA Author Manuscript

NIH-PA Author Manuscript

NIH-PA Author Manuscript

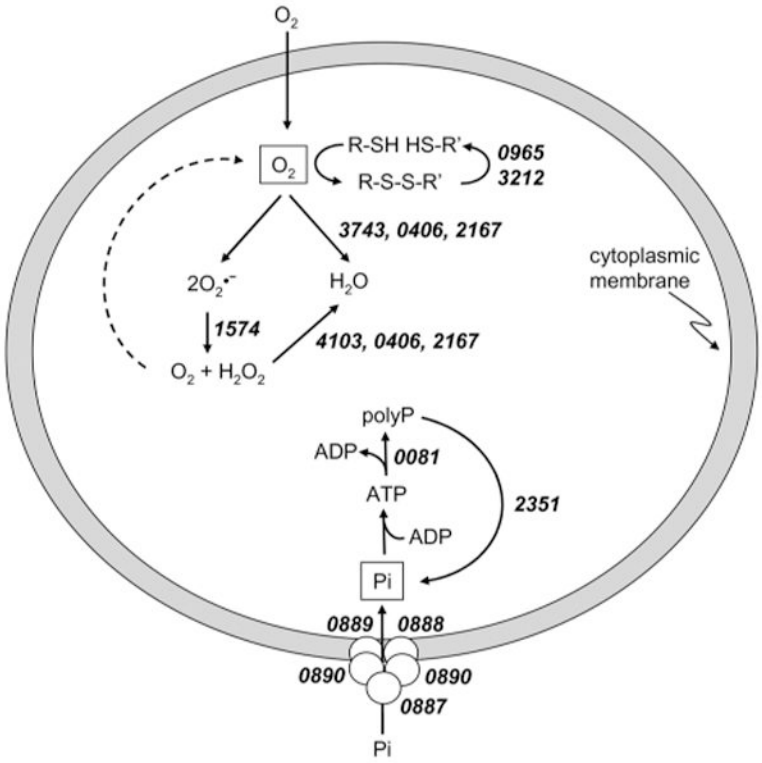

Figure 4.
Genes implicated in the stress response of acetate-grown *Methanosarcina acetivorans*. See Table 1 for gene annotations.

NIH-PA Author Manuscript

NIH-PA Author Manuscript

NIH-PA Author Manuscript

Table 1

Proteins with at least 3-fold differential abundance ratio, and genes with at least 2.5- fold differential expression ratio, in acetate- *vs.* methanol-grown *M. acetivorans*. See Table S1 for additional data.

Loci	Annotation[a]	Proteome		Transcriptome (Me/Ac)[b,e]
		No. of peptides	(Me/Ac)[b]	
MA0081	polyphosphate kinase	ND	ND	0.37
MA0133	small heat shock protein	ND	ND	0.19
MA0187	molybdenum cofactor biosynthesis protein B (MoaB)	8	5.8 ± 0.7	ND
MA0304	Molybdenum formylmethanofuran dehydrogenase (FmdE), subunit E	4	10 ± 2	ND
MA0305	Molybdenum formylmethanofuran dehydrogenase (FmdF), subunit F	4	13 ± 5	ND
MA0306	Molybdenum formylmethanofuran dehydrogenase (FmdA), subunit A	8	30 ± 10	ND
MA0307	Molybdenum formylmethanofuran dehydrogenase (FmdC), subunit C	2	30 ± 10	5.62
MA0308	Molybdenum formylmethanofuran dehydrogenase (FmdD), subunit D	3	40 ± 20	ND
MA0309	Molybdenum formylmethanofuran dehydrogenase (FmdB), subunit B	6	25 ± 9	ND
MA0368	transcriptional regulator, TetR family	4	5.8 ± 0.4	ND
MA0406	iron-sulfur flavoprotein	ND	ND	0.29
MA0455	methanol-5-hydroxybenzimidazolylcobamide co-methyltransferase (MtaC1), isozyme 1	5	500 ± 200	ND
MA0456	methanol-5-hydroxybenzimidazolylcobamide co-methyltransferase (MtaB1), isozyme 1	4	500 ± 200	ND
MA0490	sensory transduction histidine kinase	ND	ND	0.23
MA0619	sensory transduction histidine kinase	ND	ND	2.63
MA0620	sensory transduction histidine kinase	ND	ND	0.28
MA0630	groES protein (Cpn10)	ND	ND	5.33
MA0659	Na^+-transporting NADH:ubiquinone oxidoreductase, subunit 1 (Ma-RnfC)[c]	6	0.09 ± 0.04[d]	0.42
MA0660	Na^+-transporting NADH:ubiquinone oxidoreductase, subunit 2 (Ma-RnfD)[c]	ND	ND	0.40
MA0661	Na^+-transporting NADH:ubiquinone oxidoreductase, subunit 3 (Ma-RnfG)[c]	3	0.08 ± 0.03[d]	ND
MA0662	Na^+-transporting NADH:ubiquinone oxidoreductase, subunit 4 (Ma-RnfE)[c]	ND	ND	0.36
MA0663	Na^+-transporting NADH:ubiquinone oxidoreductase, subunit 5 (Ma-RnfA)[c]	ND	ND	0.26
MA0664	Na^+-transporting NADH:ubiquinone oxidoreductase, subunit 6 (Ma-RnfB)[c]	3	0.1 ± 0.03[d]	ND
MA0887	phosphate ABC transporter, solute-binding protein	3	0.01 ± 0.01	ND
MA0889	phosphate ABC transporter, permease protein	ND	ND	0.08
MA0891	phosphate transport system regulatory protein	ND	ND	0.33
MA0924	leucine responsive regulatory protein	ND	ND	2.56
MA1014	carbon-monoxide dehydrogenase, (CdhC) gamma subunit	5	0.04 ± 0.02[d]	0.11
MA1015	carbon-monoxide dehydrogenase, (CdhB) beta subunit	7	0.1 ± 0.03[d]	ND
MA1016	carbon-monoxide dehydrogenase, (CdhA) alpha subunit	6	0.04 ± 0.02[d]	0.07
MA1122	transcriptional regulator, MarR family	ND	ND	5.58
MA1189	Trp repressor binding protein	ND	ND	0.26
MA1469	response regulator receiver	ND	ND	3.51
MA1477	heat shock protein	6	13 ± 6	ND
MA1479	heat shock protein 40	ND	7 ± 2	ND
MA1487	transcription regulation protein (TetR)	ND	ND	2.57
MA1616	methanol-5-hydroxybenzimidazolylcobamide co-methyltransferase (MtaC3), isozyme 3	4	0.2 ± 0.1	0.29
MA1617	methanol-5-hydroxybenzimidazolylcobamide co-methyltransferase (MtaB3), isozyme 3	4	0.2 ± 0.1	ND
MA1682	Hsp60	ND	ND	0.13
MA1763	transcriptional regulator, CopG family	3	15 ± 4	ND

NIH-PA Author Manuscript

NIH-PA Author Manuscript

NIH-PA Author Manuscript

Loci	Annotation[a]	Proteome		Transcriptome (Me/Ac)[b,e]
		No. of peptides	(Me/Ac)[b]	
MA1799	flavodoxin	ND	ND	0.37
MA1844	sensory transduction histidine kinase	ND	ND	4.68
MA1991	sensory transduction histidine kinase	ND	ND	0.14
MA2013	sensory transduction histidine kinase	ND	ND	0.40
MA2082	sensory transduction histidine kinase	ND	ND	4.25
MA2167	iron-sulfur flavoprotein	ND	ND	0.40
MA2256	sensory transduction histidine kinase	ND	ND	0.33
MA2351	exopolyphosphatase	ND	ND	0.34
MA2699	flavodoxin	ND	ND	29.23
MA2867	polyferredoxin	2	0.08 ± 0.04	0.35
MA2914	transcriptional regulator, Hth-3 family	2	5 ± 1	2.72
MA3212	thioredoxin	ND	ND	0.14
MA3284	universal stress protein	ND	ND	0.31
MA3743	flavoprotein A	ND	ND	0.37
MA3860	carbon-monoxide dehydrogenase, (CdhA) alpha subunit	8	0.004 ± 0.002[d]	ND
MA3861	carbon-monoxide dehydrogenase, (CdhB) beta subunit	4	0.004 ± 0.002[d]	ND
MA3862	carbon-monoxide dehydrogenase, (CdhC) gamma subunit	5	0.006 ± 0.003[d]	ND
MA3863	carbon-monoxide dehydrogenase, (CooC) accessory protein	ND	ND	0.14
MA3865	carbon-monoxide dehydrogenase (CdhE), epsilon subunit	ND	ND	0.35
MA3916	nitrogen regulatory protein P-II	ND	ND	13.13
MA3972	conserved hypothetical protein	8	0.1 ± 0.06	0.13
MA4026	sensory transduction histidine kinase	ND	ND	0.16
MA4103	peroxiredoxin (alkyl hydroperoxide reductase)	ND	ND	0.34
MA4391	methanol-5-hydroxybenzimidazolylcobamide co-methyltransferase (MtaC2), isozyme 2	2	90 ± 40	ND
MA4392	methanol-5-hydroxybenzimidazolylcobamide co-methyltransferase (MtaB2), isozyme 2	2	70 ± 40	ND
MA4399	carbon-monoxide dehydrogenase, subunit alpha	ND	ND	0.27
MA4413	Hsp60	5	9 ± 4	6.03
MA4542	small heat shock protein	ND	ND	0.26
MA4566	multiple resistance/pH regulation related protein G (Na^+/H^+)	ND	ND	0.09
MA4567	multiple resistance/pH regulation related protein F (Na^+/H^+)	2	0.025 ± 0.012[d]	0.11
MA4568	multiple resistance/pH regulation related protein E (Na^+/H^+)	3	0.03 ± 0.016[d]	0.12
MA4569	multiple resistance/pH regulation related protein D (Na^+/H^+)	ND	ND	0.13
MA4570	multiple resistance/pH regulation related protein C (Na^+/H^+)	ND	ND	0.13
MA4572	multiple resistance/pH regulation related protein A (Na^+/H^+)	ND	ND	0.19
MA4671	response regulator receiver	ND	ND	0.36

[a] Annotations are those listed at http://www.tigr.org.

[b] Ac, acetate-grown cells; Me, methanol-grown cells.

[c] Originally annotated as Na^+-transporting NADH:ubiquinone oxidoreductase subunits [52], the deduced sequences were shown to have greater identity to subunits of Rnf complexes and proposed to be renamed Ma-RnfCDGEAB [30].

[d] Previously reported [30].

[e] P values were ≤0.04 (95% confidence).

ND, Not determined.

NIH-PA Author Manuscript

NIH-PA Author Manuscript

NIH-PA Author Manuscript

Table 2

Summary of proteomic and microarray expression ratios.

			Proteomic analysis	
			Methanol[a]	Acetate[b]
	Totals		184	71
Microarray analysis	Methanol[a]	210	63[c]	3[c]
	Acetate[b]	200	5[c]	17[c]

[a] Genes up regulated, or proteins in greater abundance, in methanol- *vs.* acetate-grown cells.

[b] Genes up regulated, or proteins in greater abundance, in acetate- *vs.* methanol-grown cells.

[c] Genes identified by both proteomic and microarray analysis are included in the totals shown for both analyses.

NIH-PA Author Manuscript NIH-PA Author Manuscript NIH-PA Author Manuscript

Table 3

Differentially expressed genes and differentially abundant proteins divided into functional groups.

Functional Group	Total in group[a]	Acetate-grown cells				Methanol-grown cells			
		Microarray		Proteome		Microarray		Proteome	
		Sub-total[b]	P-value	Sub-total[c]	P-value	Sub-total[b]	P-value	Sub-total[c]	P-value
RNA processing and modification	1	0	9.1E-01	0	9.57E-01	0	8.98E-01	0	8.98E-01
Chromatin structure and dynamics	1	0	9.1E-01	1	4.18E-02	0	8.98E-01	0	8.98E-01
Energy production and conversion	261	**51**[d]	**3.9E-07**	**35**	**2.37E-09**	37	1.68E-02	33	4.67E-02
Cell cycle control, mitosis and meiosis	20	3	1.7E-01	4	9.93E-03	2	2.70E-01	3	1.94E-01
Amino acid transport and metabolism	253	27	6.2E-02	7	6.22E-02	**57**	**8.27E-08**	**54**	**9.87E-07**
Nucleotide transport and metabolism	62	6	1.6E-01	4	1.50E-01	13	1.01E-02	**28**	**3.24E-10**
Carbohydrate transport and metabolism	105	15	3.1E-02	6	1.33E-01	12	1.13E-01	7	5.69E-02
Coenzyme transport and metabolism	143	14	1.1E-01	**18**	**4.52E-05**	**33**	**2.52E-05**	**32**	**6.03E-05**
Lipid transport and metabolism	32	1	1.5E-01	0	2.46E-01	6	7.33E-02	8	1.55E-02
Translation	162	9	3.0E-02	4	8.74E-02	**74**	**1.52E-25**	**83**	**7.17E-32**
Transcription	180	14	8.3E-02	4	5.99E-02	17	8.44E-02	29	8.75E-03
Replication, recombination and repair	273	***11***[e]	***4.9E-04***	***3***	***1.55E-03***	18	6.66E-03	**12**	**1.08E-04**
Cell wall/membrane biogenesis	102	8	1.2E-01	2	1.15E-01	16	3.53E-02	16	3.61E-02
Cell motility	40	3	2.1E-01	2	2.67E-01	1	5.82E-02	1	5.74E-02
Posttranslational modification, protein turnover, chaperones	116	13	9.1E-02	4	1.75E-01	14	9.77E-02	17	4.63E-02
Inorganic ion transport and metabolism	197	27	1.2E-02	9	1.34E-01	22	8.51E-02	15	3.61E-02
Secondary metabolites biosynthesis, transport and catabolism	98	11	1.0E-01	6	1.19E-01	8	1.01E-01	9	1.18E-01
General function prediction only	490	55	2.1E-02	18	7.18E-02	45	3.29E-02	65	1.20E-02
Function unknown	356	35	6.7E-02	19	6.45E-02	32	4.10E-02	29	1.99E-02

[a] Total number of genome annotations for each functional group.

[b] Number of differentially expressed genes detected for each functional group by microarray analyses.

[c] Number of differentially abundant proteins detected for each functional group by proteomic analyses.

[d] Genes shown in bold are statistically over represented.

[e] Genes shown in bold and italics are statistically under represented.